

# RSC Advances

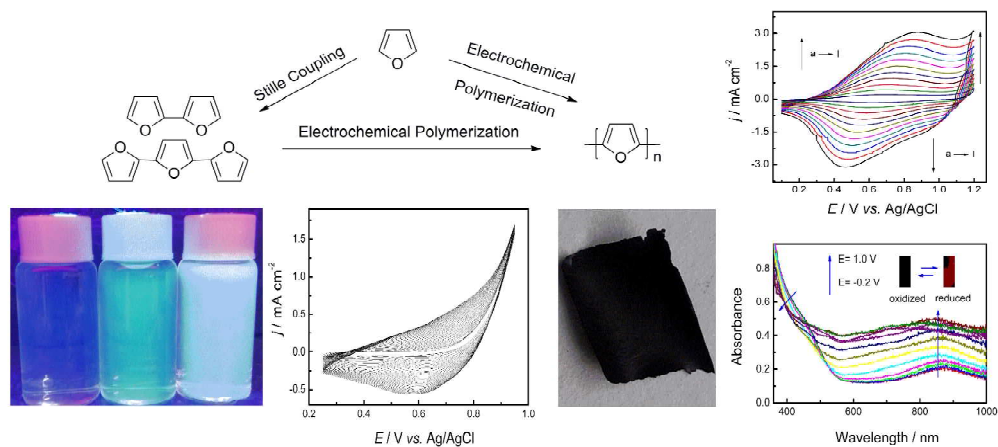


This is an *Accepted Manuscript*, which has been through the Royal Society of Chemistry peer review process and has been accepted for publication.

*Accepted Manuscripts* are published online shortly after acceptance, before technical editing, formatting and proof reading. Using this free service, authors can make their results available to the community, in citable form, before we publish the edited article. This *Accepted Manuscript* will be replaced by the edited, formatted and paginated article as soon as this is available.

You can find more information about *Accepted Manuscripts* in the [Information for Authors](#).

Please note that technical editing may introduce minor changes to the text and/or graphics, which may alter content. The journal's standard [Terms & Conditions](#) and the [Ethical guidelines](#) still apply. In no event shall the Royal Society of Chemistry be held responsible for any errors or omissions in this *Accepted Manuscript* or any consequences arising from the use of any information it contains.



Herein we demonstrated the effect of oligomer chain length on the electropolymerization and properties of the resulting polyfuran films.

Cite this: DOI: 10.1039/c0xx00000x

www.rsc.org/xxxxxx

ARTICLE TYPE

# Poly(mono-, bi- or trifuran): effect of oligomer chain length on the electropolymerization performances and polymer properties

Shijie Zhen<sup>†</sup>, Baoyang Lu<sup>†</sup>, Jingkun Xu\*, Shimin Zhang, Yuzhen Li

Received (in XXX, XXX) Xth XXXXXXXXX 200X, Accepted Xth XXXXXXXXX 200X

DOI: 10.1039/b000000x

Most recently, oligo-/polyfurans have regained widely attention due to its unique properties and promising application in organic electronics. Herein, to acquire a thorough fundamental understanding of the electrosynthesis and properties of polyfuran (PFu) from different initial oligomers, the synthesis, fluorescence, and electropolymerization performances of  $\alpha$ -oligofurans, namely furan (Fu), bifuran (2Fu), trifuran (3Fu), were comprehensively reported and the effect of oligomer chain length on the structure and properties of the resulting PFu films were evaluated. The oligofurans introduced here revealed higher fluorescence efficiency (0.05 for Fu, 0.19 for 2Fu and 0.27 for 3Fu) than the corresponding oligothiophenes and oligoselenophenes. The onset oxidation potential of oligofurans decreased obviously (1.25 V for Fu, 0.8 V for 2Fu, and 0.7 V for 3Fu) with the chain length of the starting monomers increasing, thus leading to the electrodeposition of high quality free-standing PFu films with improved optoelectronic properties. Structure characterization and properties of the as-formed PFu from different initial oligomers, including FT-IR, UV-vis, surface morphology, fluorescence, electroactivity and stability, electrochromic properties, etc., were systematically investigated and comprehensively discussed.

## 1. Introduction

Conducting polymers (CPs), an interdisciplinary research area involving close collaborations between chemists, material scientists, physicists and engineers, are still a fast-growing field in materials chemistry due to both basic scientific interest and possible commercial applications.<sup>1</sup> The field was initiated about 30 years ago by the discovery of highly conducting iodine-doped polyacetylene.<sup>2</sup> The diverse applications of conducting polymers in solar cells,<sup>3-5</sup> photovoltaic cells,<sup>6</sup> electrochromic devices,<sup>7</sup> microelectronic actuators,<sup>8</sup> light emitting diodes (LEDs),<sup>9</sup> field effect transistors (FETs),<sup>10</sup> etc., has led to much research on conjugated polyacetylenes,<sup>11</sup> polythiophenes,<sup>12-17</sup> polypyrroles,<sup>18,19</sup> poly(*p*-phenylenevinylene)s,<sup>20</sup> polyphenylenes,<sup>21</sup> and some others. Among the classical heteroaromatic polymers, polythiophenes are the most studied conducting polymers. However, despite thousands of papers published on polythiophene and its derivatives,<sup>22</sup> less attention has been focus on the study of the properties and potential applications about its close analogue, polyfuran (PFu) and its derivatives. Several possible reasons to result in the phenomenon are as follows: (a) its drastic conditions needed for polymerization and its high tendency to be

<sup>†</sup>Electronic Supplementary Information (ESI) available. See DOI: 10.1039/b0000.

overoxidized and overoxidation usually breaks the conjugation along the polymer backbone,<sup>23</sup> (b) Fu monomer and its corresponding oligofurans are unstable,<sup>24</sup> which makes it difficult to incorporate the Fu unit into conducting polymers; (c) the smaller overlap integrals and lower polarizability of oxygen atom (in Fu) compared with sulfur and selenium (in thiophene and selenophene, respectively, and their derivatives),<sup>25-26</sup> (d) Fu is known to be less aromatic than thiophene,<sup>27-30</sup> which should lead to a higher contribution from the quinoid resonance structure and might be beneficial for electron delocalization along the chain.<sup>31</sup> Given the reasons above, it is a significant challenge to prepare high-quality PFu films.

On the other hand, the promising properties of polythiophenes suggest that their oxygen analogues, PFu, should become an important member of the conducting polymer family. Considering that furan-contained polymers, such as poly{2,5-bis(2-ethylhexyl)-3-(furan-2-yl)-6-(5-(thiophen-2-yl)furan-2-yl)pyrrolo[3,4-c]pyrrole-1,4(2H,5H)-dione} PDPP2FP,<sup>3</sup> poly{3-([2,2'-bifuran]-5-yl)-2,5-bis(2-ethylhexyl)-6-(furan-2-yl)pyrrolo[3,4-c]pyrrole-1,4(2H,5H)-dione} PDPP3F,<sup>3</sup> and poly{3,6-difuran-2-yl-2,5-di(2-octyldodecyl)-pyrrolo[3,4-c]pyrrole-1,4-dione-alt-phenylene} (PDPP-FPF),<sup>32</sup> have been shown to be even better candidates for efficient solar cells and field-effect transistors than thiophene derivatives, PFu films are also expected to have some advantages over polythiophenes. Besides, PFu films have a number of other desirable properties, such as flexibility, corrosion resistance, high chemical inertness, and ease of

Jiangxi Key Laboratory of Organic Chemistry, Jiangxi Science and Technology Normal University, Nanchang 330013, China  
Tel: +86-791-88537967; Fax: +86-791-83823320;

Email: xujingkun@tsinghua.org.cn

<sup>†</sup> Mr Shijie Zhen and Mr Baoyang Lu. These authors contributed equally to this work.

processing. Importantly, biodegradable properties and availability of biorenewable sources of furan-based materials<sup>33,34</sup> could make them more fascinating than current favorites of organic materials.<sup>35,36</sup> In virtue of the potential properties of PFu and its derivatives, it is necessary to prepare high-quality PFu films and investigate their optoelectronic properties and conceivable application.

The synthesis of PFu films was firstly mentioned by G. Touillon and F. Garnier<sup>37</sup> and later by other groups<sup>38-43</sup> in order to prepare high-quality PFu films by changing experiment conditions. Recently, Fu has been used as an alternative to thiophenes in organic dyes for dye-sensitized solar cells and have shown very similar optical and electronic properties.<sup>44,45</sup> Fu-based heterocycles have also been introduced as peripheral substituents on one of the highest performing small molecules for photovoltaics.<sup>46</sup> The sparsity of studies examining polymer backbones containing Fu unit in this field is surprising, given that Fu exhibits similar energy levels and a comparable degree of aromaticity relative to their thiophene counterparts.<sup>47,48</sup> Oligofurans and furan-based molecules have been investigated by M. Bendikov<sup>49,50</sup> and S.W. Thomas group<sup>51</sup> and those materials exhibited better photovoltaic properties than oligothiophenes and its derivatives. Importantly, Fu derivatives can be synthesized from a variety of natural products; hence, they fall into the category of renewable and sustainable synthetic resources. Considering various potential applications of PFu and Fu-containing materials, the preparation and properties of PFu were necessary to investigate.

In this paper, the synthesis, fluorescence, and electropolymerization performances of oligofurans, namely furan (Fu), bifuran (2Fu), trifuran (3Fu), were comprehensively reported, and the effect of oligomer chain length on the structure and properties of the resulting PFu films obtained under optimized electrical conditions was also evaluated. Because of the drastic conditions needed for electropolymerization of Fu and less attention focused on the properties of resulting PFu films, it is very necessary and also a significant challenge to prepare high-quality PFu films. Despite the properties of thiophene (T), bithiophene (BT), trithiophene (TT),<sup>52</sup> and polythiophene<sup>12-17</sup> have been widely investigated, little is known about their properties of 2Fu and 3Fu. Besides, the resulting polymers, deriving from T, BT, and TT, revealed a steady decrease of their conjugation length as the chain length of the starting oligomers increase.<sup>52</sup> To our surprise, in contrast to those of T, BT, and TT, 3Fu and 2Fu showed better optoelectronic properties than Fu and corresponding polymer films with improved electrochemical properties were easily electrodeposited even in neutral media.

## 2. Experimental section

### 2.1 Chemicals

Furan (99%; TCI, Shanghai) was distilled under N<sub>2</sub> atmosphere twice before use. N-bromosuccinimide (NBS, 99%; Energy Chemical), *n*-butyllithium (2.5 mol L<sup>-1</sup> in hexanes; Energy Chemical), Chlorotributyltin (98%; Energy Chemical) and Tetrakis (triphenylphosphine) palladium (0) (99%; Energy Chemical) were used directly without further purification. N,N-Dimethylformamide (DMF, analytical grade; Beijing East

Longshun Chemical Plant) and Dichloromethane (DCM, analytical grade; Beijing East Longshun Chemical Plant) were purified by distillation with calcium hydride under a nitrogen atmosphere before use. Tetrabutyl-ammonium hexafluorophosphate (Bu<sub>4</sub>NPF<sub>6</sub>, 99%; Energy Chemical) was dried under vacuum at 60 °C for 24 h before use. Other chemicals and reagents (analytical grade, >98%) were all purchased commercially from Beijing East Longshun Chemical Plant (Beijing, China) and were used directly without any further treatment.

### 2.2 Monomer synthesis

Both 2,2'-bifuran (2Fu) and 2,2':5',2''-trifuran (3Fu) were synthesized as described in Scheme 1.

#### 2.2.1 Synthesis of tributyl(furan-2-yl)stannane

A solution of furan in dry THF was cooled to -78 °C, and blanked by atmosphere(Ar). *n*-BuLi (2.5 mol L<sup>-1</sup> in hexane) was slowly added dropwise. The mixture was stirred for 1~2 h at -78 °C. Then a solution of chlorotributyltin in dry THF was added slowly at the temperature of -40 °C, and the mixture was stirred for 2 h at the same temperature. After that, the temperature was warmed to room temperature, and the mixture was stirred for another 10 h under an inert atmosphere (Ar). The organic layer was dried with anhydrous MgSO<sub>4</sub> and filtered with funnel, and then this solvent was removed under reduced pressure by rotary evaporation. The stannic derivative was used without other purification for the Stille coupling reactions.<sup>53</sup>

#### 2.2.2 Synthesis of 2,2'-bifuran (2Fu)

2Fu was prepared according to literature methods.<sup>54</sup> We found this material was air-sensitive as reported by Larock.<sup>55</sup> Reddish oil, 70% yield. <sup>1</sup>H NMR (400 MHz, CDCl<sub>3</sub>), δ 6.40 (m, *J* = 4 Hz, 2H), 6.50 (d, *J* = 4 Hz, 2H) and 7.35 (d, *J* = 4 Hz, 2H) (Figure S1). <sup>13</sup>C NMR: δ 146.23, 147.17, 110.78, 104.55 (Figure S2).

#### 2.2.3 Synthesis of 2,2':5',2''-trifuran (3Fu)

2,5-Dibromofuran (0.5 g, 2.21 mmol), and tributyl(furan-2-yl)stannane (1.59 g, 4.42 mmol) were dissolved in dry DMF (40 ml) and tetrakis(triphenylphosphine) palladium (0) (50 mg, 0.443 mmol) was added at room temperature. The mixture was refluxed for 12 h at 100 °C under argon atmosphere under an inert atmosphere (Ar). Then, the mixture was cooled to room temperature, with an equal of water poured into the flask, extracted with CH<sub>2</sub>Cl<sub>2</sub>, and washed with saturated NaHCO<sub>3</sub> solution once and with water three times. The combined organic layer was dried over anhydrous MgSO<sub>4</sub> and concentrated under reduced pressure to leave a crude residue. Purification by chromatography on silica gel (EA: PE = 1:10) afforded 0.20 g 3Fu as a slightly yellow solid (46%). <sup>1</sup>H NMR (400 MHz, CDCl<sub>3</sub>), δ 6.49 (m, *J* = 4 Hz, 2H), 6.63 (t, *J* = 8 Hz, 4H), 7.45 (d, *J* = 4 Hz, 2H) (Figure S3). <sup>13</sup>C NMR: δ 146.30, 145.79, 142.02, 111.58, 107.00, 105.52 (Figure S4).

### 2.3 Electrosynthesis and electrochemical experiments

All the electrochemical experiments and polymerization of the monomers were performed in a one-compartment cell with the use of Model 263A potentiostat-galvanostat (EG&G Princeton Applied Research) under computer control. For electrochemical tests, the working and counter electrodes were both Pt wires with a

diameter of 1 mm, respectively. To obtain a sufficient amount of the polymer films for characterization, Pt sheet or ITO-coated glass with surface area of 3 cm × 2 cm were employed as the working electrode and another Pt sheet (3 cm × 2 cm) was used as the counter electrode. They were placed 5 mm apart during the examinations. Prior to each experiment, these electrodes mentioned above were carefully polished with 1500 mesh abrasive paper (for ITO: immersed in ethanol for 6 h and then cleaned by ultrasonically wave for 15 min), cleaned successively with water and acetone, and then dried in air. An Ag/AgCl electrode directly immersed in the solution served as the reference electrode, with its electrode potential calibrated against a saturated calomel electrode, and it revealed sufficient stability during the experiments. All the solutions were deaerated by a dry nitrogen stream and maintained under a slight overpressure through all the experiments to avoid the effect of oxygen.

The polymer films were grown potentiostatically at the optimized potential in CH<sub>2</sub>Cl<sub>2</sub>-Bu<sub>4</sub>NPF<sub>6</sub> (0.1 mol L<sup>-1</sup>) and its thickness was controlled by the total charge passed through the cell, which was read directly from the current-time (I-t) curves by computer. After polymerization, the polymer films were washed repeatedly with anhydrous CH<sub>2</sub>Cl<sub>2</sub> to remove the electrolyte, monomer and oligomer.

## 2.4 Characterization

<sup>1</sup>H NMR and <sup>13</sup>C NMR spectra were recorded on a Bruker AV 400 NMR spectrometer with CDCl<sub>3</sub> as the solvent and tetramethylsilane as an internal standard (TMS, singlet, chemical shift: 0.0 ppm). UV-Vis spectra of the monomers dissolved in acetonitrile were taken by using Perkin-Elmer Lambda 900 Ultraviolet-Visible Near-Infrared spectrophotometer. With an F-4500 fluorescence spectrophotometer (Hitachi), the fluorescence spectra of the monomers and polymers were determined. Infrared spectra were determined with a Bruker Vertex 70 Fourier-transform infrared (FT-IR) spectrometer with samples in KBr pellets. Scanning electron microscopy (SEM) measurements were made by using a VEGA II-LSU scanning electron microscope (Tescan) with the polymer films deposited on the ITO-coated glass. The temperature dependence of electrical conductivity of as formed P3Fu films was determined by applying a conventional four-probe technique by the use of 220 programmable current source and a Keithley 2700 multimeter under computer control.

The fluorescence quantum yields ( $\phi_{\text{overall}}$ ) of the monomers were measured using anthracene in acetonitrile (standard,  $\phi_{\text{ref}}=0.27$ )<sup>56</sup> as a reference and calculated according to the well-known method based on the expression:

$$\phi_{\text{overall}} = \frac{n^2 A_{\text{ref}} I}{n_{\text{ref}}^2 A I_{\text{ref}}} \times \phi_{\text{ref}} \quad (1)$$

Here,  $n$ ,  $A$ , and  $I$  denote the refractive index of the solvent, the absorbance at the excitation wavelength, and the intensity of the emission spectrum, respectively. Absorbance of the samples and the standard should be similar (< 0.1).

## 2.5 Electrochromic experiments

Electrochemical, spectroelectrochemical and kinetic studies were carried out on a Model 263 potentiostat-galvanostat (EG&G

Princeton Applied Research) and a Cary 50 Ultraviolet-Visible Near-Infrared spectrophotometer under computer control. Spectroelectrochemical measurements were carried out to consider absorption spectra of PFu films under the applied potential. The spectroelectrochemical cell consists of a quartz cell, an Ag wire (RE), a Pt wire (CE), and an ITO/glass as the transparent working electrode (WE). All measurements were carried out in CH<sub>2</sub>Cl<sub>2</sub>-Bu<sub>4</sub>NPF<sub>6</sub> (0.1 mol L<sup>-1</sup>). It should be noted here that the quartz cell filled with CH<sub>2</sub>Cl<sub>2</sub>-Bu<sub>4</sub>NPF<sub>6</sub> (0.1 mol L<sup>-1</sup>) and ITO-coated glass without deposited film were used as the background for spectroelectrochemical measurements.

The optical density ( $\Delta OD$ ) at the specific wavelength ( $\lambda_{\text{max}}$ ) of the sample was determined by %T values of electrochemically oxidized and reduced films, using the following equation:<sup>57</sup>

$$\Delta OD = \log(T_{\text{ox}}/T_{\text{ref}}) \quad (2)$$

The coloration efficiency (CE) is defined as the relation between the injected/ejected charge as a function of electrode area ( $Q_d$ ) and the change in optical density ( $\Delta OD$ ) at the specific dominant wavelength ( $\lambda_{\text{max}}$ ) of the sample as illustrated by the following equation:<sup>57</sup>

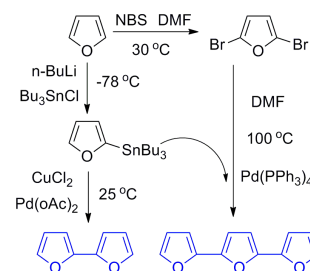
$$CE = \Delta OD/Q_d \quad (3)$$

## 2.5 Details of Computations

All calculations were carried out using the Gaussian 03 program. The structure of the oligomers were optimized without symmetry constraints using a hybrid density functional and Becke's threeparameter exchange functional combined with the LYP correlation functional (B3LYP)<sup>58</sup> and with the 6-311++G(d,p)<sup>59-62</sup> basis set (B3LYP/6-311++G(d,p)). Vibrational frequencies were evaluated at the same level to identify the real minimal energy structures.

## 3. Results and Discussion

### 3.1 Monomer synthesis



Scheme 1 Synthetic routes of 2Fu and 3Fu.

The target compounds were synthesized as shown in Scheme 1. During the synthesis of 2Fu, several attempts of the Stille coupling of tributyl(furan-2-yl)stannane with 2-bromofuran failed and the desirable compound was not obtained. Therefore, the synthesis of 2Fu is according to the literature,<sup>54</sup> and we found this material was air-sensitive as reported by Larick.<sup>55</sup> 3Fu was prepared by the usage of Stille coupling reaction of tributyl(furan-2-yl)stannane and 2,5-bibromofuran. However, it is found that 3Fu is very stable in comparison with 2Fu, even stable in air and under room temperature, which could be found in our experiments and also proved in other literature<sup>39,63-67</sup>. During the synthetic

experiments, we did meet a lot of troubles in obtaining 2Fu, for the reason that 2Fu is sensitive to air and temperature. We must adopt fast column chromatography in the purification of 2Fu and store it in refrigerator before use (4 °C). It is smoothly for us to obtain 3Fu although the yield is not much higher than others.

### 3.2 Electrochemical experiments

#### 3.2.1 Anodic polarization curves

Figure 1 shows the anodic polarization curves of 0.01 mol L<sup>-1</sup> oligofurans (Fu, 2Fu, 3Fu) in CH<sub>2</sub>Cl<sub>2</sub>-Bu<sub>4</sub>NPF<sub>6</sub> (0.1 mol L<sup>-1</sup>). The onset oxidation potentials of Fu, 2Fu, 3Fu were 1.25 V, 0.80 V, and 0.70 V (Figure 1A, B and C) vs. Ag/AgCl respectively, which were lower than those of corresponding oligothiophenes,<sup>52</sup> which might be caused by the smaller overlap integral and lower polarizability of oxygen atom compared with sulfur atom. The decrease of onset oxidation potential of oligofurans is attributed to the increase of  $\pi$ -conjugated rings of starting oligomers, making it a reality that the acquisition of PFu films at low potential. The low potential should provide considerably milder polymerization condition and yield a higher quality polymer. The differences of onset oxidation potential of oligofurans indicate the decrease of onset oxidation potential is believed to arise from an increase of the rings of  $\pi$ -conjugated oligofurans.

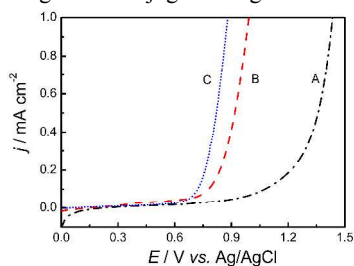


**Figure 1** Anodic polarization curves of 0.01 mol L<sup>-1</sup> Furan (A), 2Fu (B), and 3Fu (C) in CH<sub>2</sub>Cl<sub>2</sub>-Bu<sub>4</sub>NPF<sub>6</sub> (0.1 mol L<sup>-1</sup>). Potential scan rate: 50 mV s<sup>-1</sup>.

#### 3.2.2 Cyclic voltammetry (CV)

The electrochemical performances of the monomers (Fu, 2Fu, 3Fu) were examined by cyclic voltammetry (CV) in CH<sub>2</sub>Cl<sub>2</sub>-Bu<sub>4</sub>NPF<sub>6</sub> (0.1 mol L<sup>-1</sup>), as shown in Figure 2. It can be seen that CVs of Fu (Figure 2A) in this medium showed no apparent redox waves. Besides, visual inspection during CV experiments revealed that brown polymer films in a small amount were formed on the electrode after successive potential scanning, implying that the electropolymerization of Fu is difficult in CH<sub>2</sub>Cl<sub>2</sub>-Bu<sub>4</sub>NPF<sub>6</sub> (0.1 mol L<sup>-1</sup>) due to its high oxidation potential. It is interesting that CVs of 2Fu (Figure 2B) showed characteristic features of other conducting polymers during potentiodynamic synthesis such as pyrene,<sup>68</sup> and after successive potential scans, polymer films brown in color were formed on the electrodes. Furthermore, the polymerization of 3Fu reveals better redox characters than 2Fu, which can be seen from the CVs (Figure 2C), and brown polymer films were formed on the electrode by visual observation.

The broader redox waves of 3Fu (Figure 2C), compared with Fu (Figure 2A) and 2Fu (Figure 2B), may be ascribed to the wide distribution of the starting oligomer chain length.<sup>69</sup> The increase of the redox wave currents implied that the amount of the polymer films on the electrode increased. Moreover, the obvious potential shift of the wave current maximum of 3Fu (Figure 2C)

provides information about the increase in the electrical resistance of the P3Fu films and the overpotential needed to overcome this resistance. These results are usually attributed to high oxidation potential of Fu, making the electrochemical preparation of high-quality PFu films difficult. Also, the resulting P3Fu and P2Fu showed improved optoelectronic properties with the chain length of the starting monomers increasing.

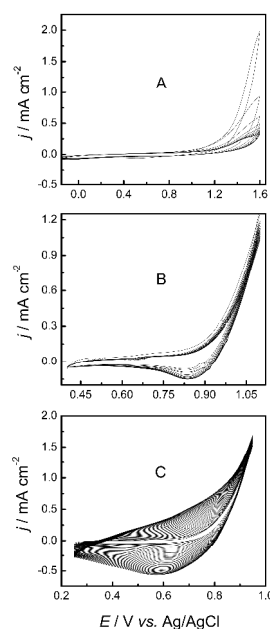


**Figure 2** CVs of 0.01 mol L<sup>-1</sup> Furan (A), 2Fu (B), and 3Fu (C) in CH<sub>2</sub>Cl<sub>2</sub>-Bu<sub>4</sub>NPF<sub>6</sub> (0.1 mol L<sup>-1</sup>). Potential scan rate: 100 mV s<sup>-1</sup>.

#### 3.2.3 Optimization of electrical conditions and preparation of PFu films

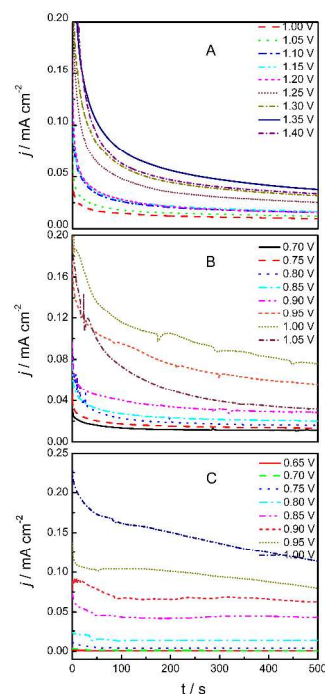


**Figure 3** Chronoamperograms of 0.01 mol L<sup>-1</sup> Furan (A), 2Fu (B), and 3Fu (C) in CH<sub>2</sub>Cl<sub>2</sub>-Bu<sub>4</sub>NPF<sub>6</sub> (0.1 mol L<sup>-1</sup>) on Pt electrode at different applied potentials for 500 s.

The deposition potential significantly influences the structure and properties of conjugated polymer as various FTIR studies have demonstrated.<sup>70,71</sup> To optimize applied potentials for electropolymerization, a set of current transients during the electropolymerization of oligofurans at different applied potentials in CH<sub>2</sub>Cl<sub>2</sub>-Bu<sub>4</sub>NPF<sub>6</sub> (0.1 mol L<sup>-1</sup>) were recorded, as shown in Figure 3. Considering the overall factors affecting the quality of the as-formed polymer films, such as moderate polymerization rate, negligible overoxidation, regular morphology, and good adherence against the working electrode, the optimized applied potentials of Fu, 2Fu, and 3Fu were 1.4 V (Figure 3A), 0.9 V (Figure 3B), and 0.8 V (Figure 3C) vs. Ag/AgCl, respectively. Therefore, PFu, P2Fu, and P3Fu films used for the characterization mentioned below were all prepared by the chronoamperometry method at constant potentials of 1.4 V, 0.9 V, and 0.8 V, respectively. Also, visual inspection demonstrated that PFu, P2Fu and P3Fu films with smooth, homogeneous, and continuous surfaces were formed at applied potentials of 1.4 V, 0.9 V, and 0.8 V, as predicted from their I-t curves (Figure 3A, B and C), and they showed good adherence against the electrode.

### 3.2.4 Electrochemistry of PFu films

The electrochemical properties of PFu films have not been well-characterized compared with other typically conducting polymers, such as polythiophene and polypyrrole, since PFu prepared directly from the electrochemical oxidation of Fu showed poorly defined properties.<sup>39,72-74</sup> In order to get a deeper insight into the electrochemical activities and environmental stability of as-formed polymer films, the electrochemical behaviors of PFu, P2Fu and P3Fu by cyclic voltammetry in monomer-free CH<sub>2</sub>Cl<sub>2</sub>-Bu<sub>4</sub>NPF<sub>6</sub> (0.1 mol L<sup>-1</sup>) were investigated, as shown in Figure 4.

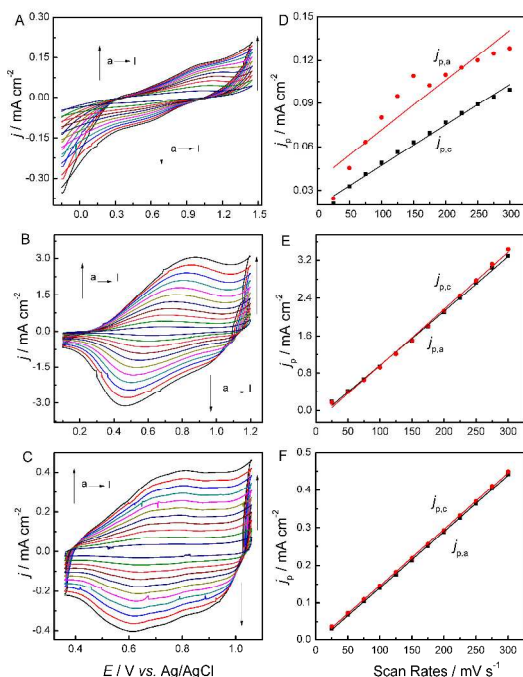


**Figure 4** CVs of PFu, P2Fu and P3Fu films in monomer-free CH<sub>2</sub>Cl<sub>2</sub>-Bu<sub>4</sub>NPF<sub>6</sub> (0.1 mol L<sup>-1</sup>) at potential scan rates of (a) 25 mV s<sup>-1</sup>, (b) 50 mV s<sup>-1</sup>, (c) 75 mV s<sup>-1</sup>, (d) 100 mV s<sup>-1</sup>, (e) 125 mV s<sup>-1</sup>, (f)

150 mV s<sup>-1</sup>, (g) 175 mV s<sup>-1</sup>, (h) 200 mV s<sup>-1</sup>, (i) 225 mV s<sup>-1</sup>, (j) 250 mV s<sup>-1</sup>, (k) 275 mV s<sup>-1</sup>, (l) 300 mV s<sup>-1</sup>. Right of the figure: plots of redox peak current densities vs. potential scan rates.  $j_p$  is the peak current density, and  $j_{p,a}$  and  $j_{p,c}$  denote the anodic and cathodic peak current densities, respectively.

The potentials needed to oxidize and reduce the polymer films were from 1.05 V (anodic peak potential, E<sub>a</sub>) to 0.55 V (cathodic peak potential, E<sub>c</sub>) vs. Ag/AgCl for PFu (Figure 4A), from 0.88 V to 0.45 V for P2Fu (Figure 4B), and from 0.81 V to 0.60 V (Figure 4C) in monomer-free CH<sub>2</sub>Cl<sub>2</sub>-Bu<sub>4</sub>NPF<sub>6</sub> (0.1 mol L<sup>-1</sup>). As the oxidation potential can be related to the extent of conjugation in the polymers, these results suggested an increase of mean conjugation length from PFu to P3Fu.<sup>75</sup> The driving voltage for P3Fu is lower than those of PFu and P2Fu. The differences, corresponding with the highest occupied states in the valence band,<sup>76</sup> were commonly observed in the electrochemistry of conducting polymers and may be due to a number of factors including the ease of diffusion of dopant ions in and out of the film or interfacial charge transfer process. Furthermore, the main reasons accounting for the shift of redox peaks among CV curves (Figure 4) for polymer films are usually as follows:<sup>77</sup> slow heterogeneous electron transfer, local rearrangement effect of polymer chains, slow mutual transformation of various electronic species, and electronic charging of interfacial exchange corresponding to the metal/polymer and polymer/solution interfaces, etc. PFu film derived from Fu presented bad linearity between peak current densities and potential scanning rates (Figure 4D), while the peak current densities were proportional to potential scanning rates for P2Fu and P3Fu (Figure 4E and F), indicating that the redox process is nondiffusional and the electroactive polymers is well adhered to the working electrode surface.<sup>78</sup> Compared the above results, we can conclude that the electropolymerization at low potential, with the chain length of the starting oligofurans increasing, lead to electrodeposition of high-quality polymer films.

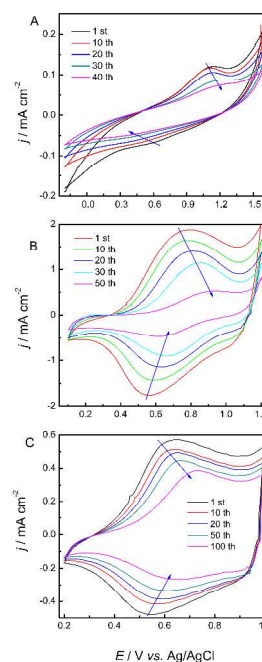
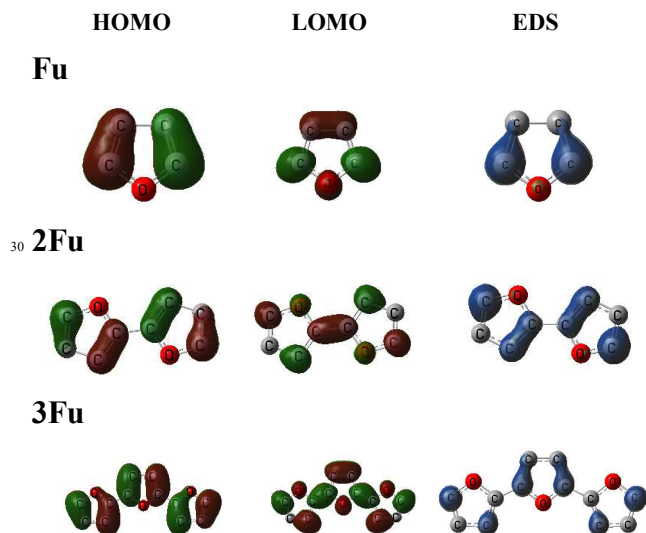


**Figure 5** CVs of PFu (A), P2Fu (B) and P3Fu (C) films in monomer-free  $\text{CH}_2\text{Cl}_2\text{-Bu}_4\text{NPF}_6$  ( $0.1 \text{ mol L}^{-1}$ ) at the potential scan rate of  $150 \text{ mV s}^{-1}$ .

It is well known that the good stability of conducting polymers is very significant for their applications in electronic devices.<sup>10</sup> Therefore, the long-term stability of the redox activity of PFu, P2Fu and P3Fu was also investigated to evaluate the electrochemical stability of the polymer films in  $\text{CH}_2\text{Cl}_2\text{-Bu}_4\text{NPF}_6$  ( $0.1 \text{ mol L}^{-1}$ ), as shown in Figure 5. It is obviously that CVs of PFu in this medium (Figure 5A) showed no apparent redox waves, so the stability of redox activity of PFu is not necessary to investigate. Compared to PFu, the amount of exchange charge of P2Fu was remaining 22.8% after 50 cycles (Figure 5B), while P3Fu had about 71.8% of electrochemical activity after 50 cycles (Figure 5C). Also, After completion of 100 cycles, the stability of P3Fu exhibited only 57.4% of electrochemical activity. P3Fu presented better electrochemical activity than P2Fu and PFu. Furthermore, P2Fu and P3Fu could be cycled repeatedly between the conducting (oxidized) and insulating (neutral) state without significant decomposition, indicating the relatively good redox stability of those materials. All these electrochemical experiments indicated that 2Fu and 3Fu, by increasing the chain length of starting oligomers, lead to successful electrodeposition of high-quality PFu films.

### 3.3 Structural characterization and properties

#### 3.3.1 Computational results



**Scheme 2** HOMO and LUMO orbitals of the oligofurans and isovalent surfaces of electron spin densities for their radical cations.

To aid in understanding the chemical structures of the resulting films, DFT (density functional theory) calculations for oligofurans, namely furan (Fu), bifuran (2Fu) and trifuran (3Fu), were carried out and analyzed for the structural study of PFu films at B3LYP/6-311G\* level. Their frontier orbitals (HOMO and LUMO) and atomic electron spin densities (ESD) were all shown in Scheme 2. During the electropolymerization, a necessary step is that the oxidation reaction leads to the ionization of molecules and to the formation of a radical cation. The polymerization is believed to proceed through the  $\alpha$  positions of the external heterocyclic rings. The furan atom with negative charge

will donate electrons during electrochemical polymerization and reactions between active molecules mainly occur on the frontier molecular orbital and the near orbital according to the molecular orbital theory. For all the molecules, the negative electric charges mainly concentrated on C-H bonds. However, no significant difference was observed for the reactivity of  $\alpha$  and  $\beta$  sites on the furan rings. The calculated molecular orbitals of these oligomers demonstrated that the HOMO proportions of the  $\alpha$  sites were higher than those of other atoms (Scheme 2). This means that the conjugated structure of the formed oligomers result in a decrease in the relative reactivity of the proposed positions, which probably caused a decrease or even in some cases a complete loss of polymerizability. Also, the polymerization would happen preferentially at C(2) and (7) positions of oligofurans due to their much higher ESD (Scheme 2) than other positions.<sup>79,80</sup> It can be reasonably deduced that the polymerization sites of these compounds are preferentially  $\alpha$  positions.

#### 3.3.2 UV-vis spectra of PFu films

The optical properties of conjugated polymers are generally characterized by a wide absorption band due to intrinsic energetic disorder in these polymers. A broad absorption means a wider distribution of the conjugation lengths in the polymer.<sup>72</sup> Therefore, UV-vis spectra of the oligofurans in acetonitrile and polymers electrodeposited on ITO were examined, as shown in Figure 6 and Figure 9. Fu and 2Fu showed a characteristic absorbance peak at 213 nm (Figure 6A) and 281 nm (Figure 6B), while 3Fu at 328 nm (Figure 6C), which were assigned to a single electron  $\pi\text{-}\pi^*$  transition of aromatic rings.<sup>81</sup> The bathochromic shift between the maximum absorption of oligofurans indicated that 2Fu and 3Fu have a longer chain sequence than Fu. The UV-vis spectra of PFu, P2Fu and P3Fu films were described in the part of spectroelectrochemical studies.

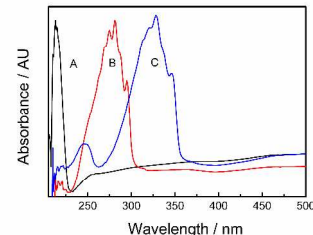


**Figure 6** UV-vis spectra of Furan (A), 2Fu (B), and 3Fu (C) in acetonitrile.

#### 3.3.3 Fluorescence spectra of the oligofurans and their corresponding polymers

The fluorescence emission spectra of oligofurans in acetonitrile and doped polymers electrodeposited on ITO-coated glass were determined, as shown in Figure 7. The emission spectrum of Fu (Figure 7A) emerged at 457 nm when excited at 382 nm whereas a maximum emission peak at 509 nm characterized the spectrum of doped PFu (Figure 7D) when excited at 251 nm. For 2Fu (Figure 7B), it exhibited a strong emission peak at 466 nm under excitation at 398 nm, and the emission of P2Fu (Figure 7E) centered at 582 nm at 288 nm excitation. A dominant maximum emission at 509 nm of 3Fu when excited at 404 nm, while doped P3Fu exhibited a maximum emission peak at 608 nm (Figure 7F) at 301 nm excitation. Slightly red shifts among the oligofurans (about 9 nm between Fu and 2Fu and 43 nm between 2Fu and 3Fu) can be seen from Figure 7, which is mainly attributable to elongation of the oligofurans' delocalized  $\pi$ -electron chain sequence. Large red shifts between the oligofurans and polymers (52 nm between Fu and PFu and 116 nm between 2Fu and P2Fu and 99 nm between 3Fu and P3Fu) are obviously exhibited in

Figure 7, resulting from the enhancement of the delocalization of  $\pi$ -electron. The differences of the maximum emission among the polymers (509 nm for PFu, 582 nm for P2Fu, and 608 nm for P3Fu) are mainly attributed to the chain length of the obtained polymer films.

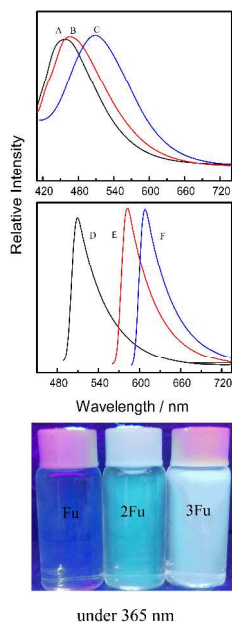


**Figure 7** Fluorescence spectra of monomers in acetonitrile and polymers deposited electrochemically on the ITO coated glass as indicated and photoluminescence of monomers in acetonitrile under 365 nm UV irradiation: Furan (A), 2Fu (B), 3Fu (C), PFu (D), P2Fu (E) and P3Fu (F).

According to equation 1, the fluorescence quantum yield ( $\phi_{overall}$ ) of Fu in acetonitrile was calculated to be 0.05, while those of the 2Fu and 3Fu prepared in acetonitrile were 0.19 and 0.27, respectively. These data of oligofurans were much higher than those of corresponding oligothiophenes (bithiophene: 0.013, and trithiophene: 0.056).<sup>81</sup> The better regioregularity and more uniform structure of oligofurans, reducing the fluorescence quenching, made them exhibit much higher fluorescence quantum yield. Another reason for this phenomenon is apparently due to the high rigidity, decreasing out-of-plane vibrations and quinoid character of the oligofurans.<sup>72</sup> Meanwhile, it is also very interesting to find that 2Fu and 3Fu dissolved in common organic solvents, such as methanol, ethanol, acetone, acetonitrile, diethyl ether, dimethyl sulfoxide, etc., can all emit strong blue-green photoluminescence when exposed to 365 nm UV light, as shown in Figure 7.

Based on the fluorescence results, 2Fu and 3Fu showed good blue-green light-emitting properties, and it can be expected that they may be used as fluorescence materials and electroluminescent materials.

### 3.3.4 FT-IR Spectra of the monomers and polymers

FT-IR spectra of PFu films were first reported by G. Zotti et al.<sup>38</sup> However, the spectra of PFu directly derived from Fu monomer has always been poorly defined due to saturated-ring moieties in the polymer chains. In order to elucidate the structures of the monomers and corresponding polymers, FT-IR spectra of a series of oligofurans and PFu films were recorded, as shown in Figure 8.

As can be seen from Figure 8, the absorption bands in the spectra of the doped polymers were obviously broadened in comparison with those of the monomers, similar to those of other conducting polymers reported previously,<sup>82-85</sup> which may be attributable to the wide conjugated chain length distribution of polymers.

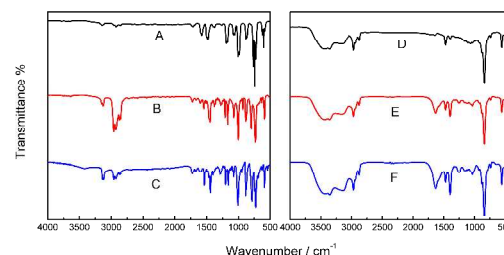


**Figure 8** FT-IR spectra of Furan (A), 2Fu (B), 3Fu (C), PFu (D), P2Fu (E) and P3Fu (F).

The absorption at 796  $\text{cm}^{-1}$  (Figure 8B), 790  $\text{cm}^{-1}$  (Figure 8C), 878  $\text{cm}^{-1}$  (Figure 8D), 879  $\text{cm}^{-1}$  (Figure 8E), and 879  $\text{cm}^{-1}$  (Figure 8F) are characteristic of the  $\alpha$ - $\alpha$  coupling of the carbon backbone, namely head to tail coupling,<sup>88</sup> indicating the electropolymerization preferentially occurred at the 2,5-positions<sup>89,90</sup> and main component in polymers is conjugated.<sup>39</sup> The appearance of characteristic absorptions due to the aromatic ring stretching mode located at 1471  $\text{cm}^{-1}$  (Figure 8D), 1473  $\text{cm}^{-1}$  (Figure 8E) and 1473  $\text{cm}^{-1}$  (Figure 8F) indicate that most of the Fu rings in the polymer chains remain intact.<sup>39</sup> The band of doped anion  $\text{PF}_6^-$  are assigned at 842  $\text{cm}^{-1}$ . Interestingly, the strong and broad absorption emerged at 3500  $\text{cm}^{-1}$  in the spectra of both PFu, P2Fu, and P3Fu (Figure 8D, E and F) compared with the spectra of the monomers, indicating the existence of O-H in the polymer. This may be ascribed to the proton-doping properties of the polymers, and the proton dopants come from the deprotonization of the radical cations during the electrochemical polymerization.<sup>91</sup> Figure 8D, E, and F show a strong absorption in aliphatic C-H stretching vibration region (bands located at 2972-2872  $\text{cm}^{-1}$ ) and a strong absorption located at  $\sim 1640$   $\text{cm}^{-1}$  (Figure 8E and F) indicating the existence of C=O bonds, which suggests the ring-opening reaction. The relatively high frequency of the C=O stretching vibrations may be due to the fact that there are ring openings adjacent to one another thus destroying conjugation with the furan ring. Additional bands shown in the FTIR of the polymers at 1157  $\text{cm}^{-1}$  (Figure 8F), 1250  $\text{cm}^{-1}$  (Figure 8E and F), and 1031  $\text{cm}^{-1}$  (Figure 8D, E and F) were attributed to C-H bending and stretching.<sup>68</sup> Besides, the presence of  $\nu(\text{C-H})$  at 3100  $\text{cm}^{-1}$  indicated that the material produced was polyconjugated PFu.<sup>92</sup>

The usage of Fu unit, during the electrochemical polymerization, resulted in that the ring opening reaction is more extensive than 2Fu and 3Fu, which is due to high threshold voltage required for the electropolymerization. By increasing the rings of starting oligofurans, the onset oxidation potential of monomers can be lowered, then the desired high-quality PFu films can be obtained. This is in well accordance with those results in electrochemical data.

### 3.4 Electrochromic properties

Thin polymer films were electrochemically deposited on transparent ITO-coated glass plates potentiostatically at the optimal potential of the oligofurans. The potential applied to the polymer-coated electrode was initially in the fully reduced state and then sequentially increased to higher potentials to oxidize the polymer while monitoring the creation of the charge carriers. The reversibility of the electronic structure of the polymers was then tested by examining the spectra as the polymers were switched from the oxidized to the reduced form. The optical band gap for each polymer was obtained from the onset of  $\pi$ - $\pi^*$  transition. Oxidation of the polymer leads to the formation of polaronic charge carriers and induces a change in the polymer conformation to a quinoidal structure. From Figure 9, stepwise oxidation of P2Fu showed the slightly fading of absorbance at 420 nm and typical evolution of peaks at more than 700 nm,<sup>93</sup> while those of P3Fu were 450 nm and 820 nm, respectively. Moreover, the corresponding colors of PFu were gray in the reduced state and pale in the oxidized state (Figure 9A, inset), while P2Fu exhibited yellowish-green in the reduced state and gray in the oxidized state, and P3Fu showed brownish in the reduced state and dark in the oxidized state (Figure 9B and C, insert).

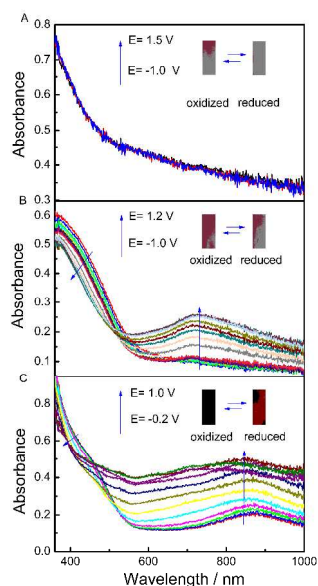


**Figure 9** Spectroelectrochemistry of PFu, P2Fu and P3Fu films electropolymerized on ITO coated glass in monomer-free  $\text{CH}_2\text{Cl}_2$ - $\text{Bu}_4\text{NPF}_6$  ( $0.1 \text{ mol L}^{-1}$ ).

These spectra revealed an apparently bathochromic shift of the absorption maximum of P2Fu ( $\lambda=725 \text{ nm}$ ) when compared with P3Fu ( $\lambda=850 \text{ nm}$ ), indicating a higher conjugation for P3Fu.<sup>75</sup> Obviously, the spectra of PFu showed no visible absorbance, demonstrating a lower conjugation of PFu than P2Fu and P3Fu. These data of the absorbance of polymers confirmed that the mean conjugation length in the polymers increase steadily when increasing the chain length of the starting oligomers, in agreement with the trend expressed by the electrochemical data reported above. Besides, in accordance with the conclusion of recent publications,<sup>94,95</sup> our results clearly showed that using oligomers of increasing chain length as starting materials leads finally to the expected result, giving more conductive polymers with a higher degree of conjugation.<sup>75</sup>

Band gaps of PFu, P2Fu and P3Fu, for a direct interband transition, which can be estimated from the absorption edge ( $\sim 580 \text{ nm}$  of P3F,  $\sim 569 \text{ nm}$  of P2F and  $\sim 515 \text{ nm}$  of PFu) of the spectra ( $\sim 515 \text{ nm}$  of PFu,  $\sim 569 \text{ nm}$  of P2Fu, and  $\sim 580 \text{ nm}$  of P3Fu), were about 2.41 eV, 2.18 eV and 2.14 eV, respectively. They were higher than that of neutral PFu (2.07 eV) reported by Wan et al.,<sup>83</sup> and lower than that of undoped PFu (2.7 eV) reported by Oshawa et al.<sup>42</sup> It should be noted that the calculated band gap value of PFu is about 6.5 eV,<sup>96</sup> which is much higher than the experimental one. Band gaps of P2Fu and P3Fu, which were slightly higher than that of PFu, were probably due to a more ordered structure of electrodeposited polymers. The experimental band gap of PFu was higher than that of polythiophene (2.04 eV)<sup>97</sup> and polyselenophene (2.1 eV),<sup>98,99</sup> and lower than that of polypyrrole (2.85 eV). This phenomenon can be explained by the weak  $\pi$ -donor strengths of the heteroatoms, which can be achieved in going to higher periods or to the left in the Periodic Table.<sup>100</sup>

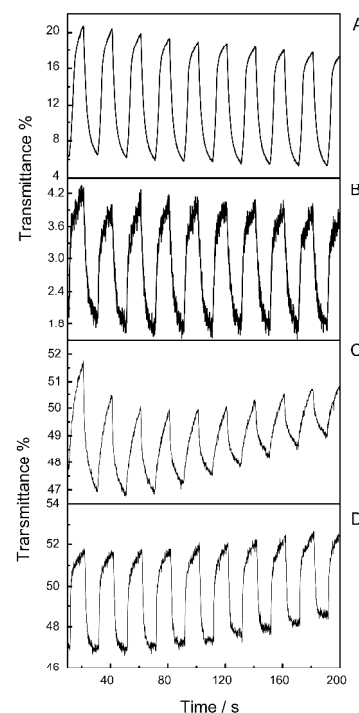


**Figure 10** Transmittance-time at specific wavelength profiles of P3Fu film (A and B) recorded during double step spectrochronoamperometry between -0.6 V and 0.8 V and P2Fu film (C and D) recorded during double step spectrochronoamperometry between -0.5 V and 0.8 V for the switching time of 10 s as indicated: A: 650nm; B: 990 nm; C: 725 nm and D: 990nm.

The optical switching studies of PFu, P2Fu and P3Fu were carried out using a square wave potential step method coupling with optical spectroscopy known as chronoabsorptometry in a monomer-free  $\text{CH}_2\text{Cl}_2$ - $\text{Bu}_4\text{NPF}_6$  ( $0.1 \text{ mol L}^{-1}$ ) solution. The electrochromic parameters, such as optical contrast ratio ( $\Delta T\%$ ), response time and coloration efficiency of the polymer films, were investigated by increment and decrement in the transmittance with respect to time at the specific absorption wavelength, as shown in Figure 10. The potentials were

switching alternatively between the reduced and oxidized states with the residence time of 10 s. Electrochromic parameters of P2Fu and P3Fu films are listed in Table 1. The electrochromic parameters of PFu were not obtained for the reason that the obtained PFu has no optical contrast ratios, which can be seen from its Spectroelectrochemistry.

The optical contrast ratios of P2Fu films between neutral and oxidized state were calculated to be 4.15% and 4.4% at 725 nm and 980 nm, respectively (Figure 10A and B). For P3Fu films, the optical contrast ratios were found to be 13.31% at 650 nm and 2.32% at 990 nm (Figure 10C and D). The difference is attributed to the effect of starting oligofurans chain length. Furthermore, the  $\Delta T\%$  values are quite low among other electrochromic conducting polymers,<sup>101</sup> leading to their low coloration efficiency values.

Response time is an important parameter for a polymer since it indicates the speed of ions moving into the polymer chains during the doping process. Like most electrochromic conducting polymers, the oxidation state from the neutral state of P2Fu and P3Fu films (coloration step) proceeds more slowly than the reduction of the oxidized form (bleaching step) due to the difference in charge transport rates between the two states. The

response time required to attain 95% of total transmittance difference were found to be 3.9 s at 980 nm for P2Fu films and 5.3 s at 990 nm for P3Fu films and from the reduced state to the oxidized state, while from the oxidized state to the reduced state, the response time was 3.7 s at 980 nm for P2Fu films and 4.7 s at 990 nm for P3Fu films, respectively.

The coloration efficiency (CE) is also an important characteristic for electrochromic materials and obtained for a certain amount of the charge injected in the polymer films as a function of the change in optical density. In this study, the coloration efficiency (CE) P2Fu films to be 51.8  $\text{cm}^2 \text{C}^{-1}$  at 990 nm and 85.1  $\text{cm}^2 \text{C}^{-1}$  at 980 nm, which is slightly different to that of the P3Fu films, whose CE is measured as 99.9  $\text{cm}^2 \text{C}^{-1}$  at 650 nm and 47.6  $\text{cm}^2 \text{C}^{-1}$  at 990 nm. The difference between P2Fu and P3Fu is attributed to the length of the starting oligofurans. Furthermore, the CE of P2Fu and P3Fu are lower than those of corresponding polythiophene, which might be caused by the differences in atomic radius and electronegativity between oxygen and sulfur atoms. By considering all the above data concerning electrochromic properties, we can draw the conclusion that the electrochromic properties of resulting PFu films were based on the length of the starting oligofurans.

**Table 1** Electrochromic parameters of P2Fu films and P3Fu films

Polymer	Wavelength / nm	$T_{\text{red}}$	$T_{\text{ox}}$	$\Delta T$	response time (s)		coloration efficiency ( $\text{cm}^2/\text{C}$ )
					oxidation	reduction	
P(3Fu)	650	7.3	20.6	13.3	6.0	5.6	99.9
	990	4.1	1.8	2.3	5.3	4.7	47.6
P(2Fu)	980	51.7	47.3	4.4	3.9	3.7	85.1
	725	47.6	51.7	4.2	7.4	3.2	51.8

### 3.5 Morphology of the PFu films

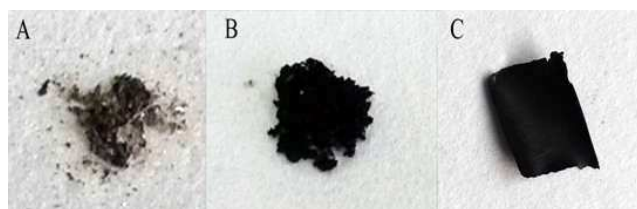


**Figure 11** Samples of PFu (A), P2Fu (B) and P3Fu (C) by electropolymerization in  $\text{CH}_2\text{Cl}_2\text{-Bu}_4\text{NPF}_6$  ( $0.1 \text{ mol L}^{-1}$ ).

Photographs of PFu, P2Fu and P3Fu obtained by electropolymerization in  $\text{CH}_2\text{Cl}_2\text{-Bu}_4\text{NPF}_6$  ( $0.1 \text{ mol L}^{-1}$ ), as shown in Figure 11. PFu is in the form of brown powder (Figure 11A) and P2Fu is black powder (Figure 11B), while P3Fu is metallic black free-standing film (Figure 11C). This could be ascribed to the lowering of oxidation potentials, which has been shown to be an effective way to decrease the degree of alpha-beta coupling reactions. Polymerization at low potential resulted in smooth, homogeneous polymer films. As the chain length of the starting oligomer increased, the microscopy of the corresponding polymers became better (P3Fu > P2Fu > PFu). Compared with previous results<sup>102</sup>, P3Fu films prepared at low voltage effectively avoid surface morphology changes caused by side-chain

cross-linking, which could lead to main chain distortion<sup>102</sup>. In view of this, the degree of conjugation of P3Fu is higher than those of P2Fu and PFu, partly indicating the electropolymerization of furan-based monomers mainly occurred at alpha site, namely  $\alpha\text{-}\alpha$  coupling of the carbon backbone. It should be noted here that the polymers were electrosynthesis in neutral media.

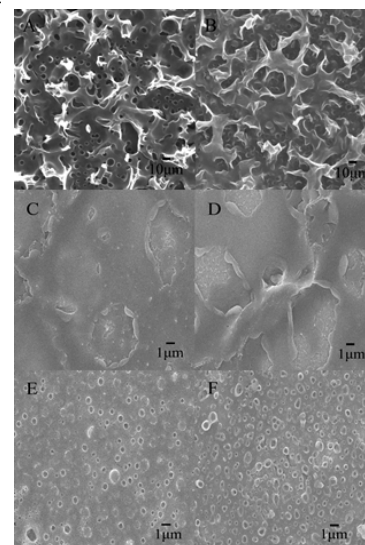


**Figure 12** SEM photographs of PFu, P2Fu, and P3Fu deposited electrochemically on the ITO electrode: doped (A) and dedoped (B) PFu; doped (C) and dedoped (D) P2Fu; doped (E) and dedoped (F).

Scanning electron microscopy has been one of the most widely used techniques in the study of the morphology of polymeric materials for analyzing their constituents and texture. Besides, surface microscopy of conducting polymers are closely related to their properties, such as electrical conductivity, redox activity and stability. Therefore, the surface morphology of PFu, P2Fu, and P3Fu films deposited on the ITO electrodes were investigated by scanning electron microscope (SEM) as shown in Figure 12. Macroscopically, even at high magnifications, PFu films appeared to be laminar porous structure (Figure 12A and B), and the dedoped PFu showed a homogeneous structure with holes (Figure 12B), indicating the counter anions migrating out of the polymer films. The obtained P2Fu and P3Fu films, with the increase of the length of starting oligomers, exhibited smoother and more homogeneous structure (Figure 12C and E) than PFu films (Figure 12A). Similarly, dedoped P2Fu and P3Fu films presented porous structure (Figure 12D and F). This laminar porous structure could account for the low value of the P3Fu films conductivity and its increase with the degree of hydration as Oshawa et al. established.<sup>42</sup>

### 3.6 Electrical conductivity of free-standing P3Fu

The electrical conductivity of the obtained free-standing P3Fu film (Figure 11C) were tested and the value was determined to be about  $6 \times 10^{-4}$  S/cm, much lower than that of doped PFu ( $10^{-2}$  S/cm) reported in ref.,<sup>40</sup> which was prepared in boron trifluoride diethyl etherate (BFEE). However, the dopants ( $[(C_2H_5)_3O^+ BF_4^-]$ ) in the resulting polymers are volatile and water-sensitive, making the doped state of the polymers very unstable. Importantly, PFu films derived from oligofuran in BFEE were also prepared, but little of PFu films were obtained due to the instability of 2Fu and 3Fu in lewis acid of BFEE. The low electrical conductivity of the P3Fu films may be attributed to the shorter conjugation length compared with polypyrrole and polythiophene and the unfavorable electronic effects of the oxygen atom.<sup>103</sup> Another reason is that the ring-opening reaction cannot be totally suppressed in this solvent system, and nonconjugated regions exist in the polymer, although in small amounts. As a consequence, the existence of lower electrical conductivity domains in the film restricts the charge carrier migration in the polymer.<sup>104,105</sup>

## 4. Conclusions

In summary, we have introduced a class of organic materials, namely, oligofurans and PFu, which fulfill the most important requirements for a wide range of applications. The electropolymerization performances of a series of oligofurans, including Fu, 2Fu and 3Fu, have been systematically investigated and obtained P2Fu and P3Fu films reveals better reversible redox activities and reversible electrochromic properties. The oligofurans introduced here combine higher fluorescence and greater process ability than the corresponding oligothiophene. A free-standing P3Fu film electropolymerized from 3Fu, exists relatively high electrical conductivity as  $6 \times 10^{-4}$  S/cm, at room temperature. Importantly, Fu-based materials should be biodegradable and can be obtained directly from renewable

resources. Although these results of PFu are not very attracting in comparison with those of polythiophenes, high-quality PFu films with improved optoelectronic properties with the chain length of starting monomers increasing, making PFu family the potential application of in organic electronic application in the future.

## Acknowledgement

We are grateful to the National Natural Science Foundation of China (grant number 51303073), and the Natural Science Foundation of Jiangxi Province (grant number 20122BAB216011), and Jiangxi Science and Technology Normal University (Ky2012zy07) for their financial support of this work. Thanks are also due to Associate Prof. Dr. Guangming Nie for his kind assistance on the electrochromic tests.

## References

- T. A. Skotheim and J. R. Reynolds, Handbook of Conducting Polymers, CRC Press, Taylor & Francis Group, Boca Raton, 2007.
- H. Shirakawa, E. J. Lewis, A. G. MacDiarmid, C. K. Chiang and A. J. Heeger, *J. Chem. Soc. Chem. Commun.*, 1977, **16**, 578-580.
- C. H. Woo, P. M. Beaujuge, T. W. Holcombe, O. P. Lee and J. M. J. Fréchet, *J. Am. Chem. Soc.*, 2010, **132**, 15547-15549.
- A. T. Yiu, P. M. Beaujuge, O. P. Lee, C. H. Woo, M. F. Toney and J. M. J. Fréchet, *J. Am. Chem. Soc.*, 2012, **134**, 2180-2185.
- J. C. Bijleveld, B. P. Karsten, S. G. J. Mathijssen, M. M. Wienk, D. M. de Leeuw and R. A. J. Janssen, *J. Mater. Chem.*, 2011, **21**, 1600-1606.
- C. J. Brabec, N. S. Sariciftci and J. C. Hummelen, *Adv. Funct. Mater.*, 2001, **11**, 15-26.
- S. I. Cho, W. J. Kwon, S. Choi, P. Kim, S. Park, J. Kim, S. J. Son, R. Xiao, S. Kim and S. B. Lee, *Adv. Mater.*, 2005, **17**, 171-175.
- M. J. Marsella, R. J. Reid, S. Estassi and L. S. Wang, *J. Am. Chem. Soc.*, 2002, **124**, 12507-12510.
- I. F. Perepichka, D. F. Perepichka, H. Meng and F. Wudl, *Adv. Mater.*, 2005, **17**, 2281-2305.
- H. E. Katz, *Chem. Mater.*, 2004, **16**, 4748-4756.
- J. W. Y. Lam and B. Z. Tang, *Acc. Chem. Res.*, 2005, **38**, 745-754.
- G. E. Gunbas, A. Durmus and L. Toppare, *Adv. Mater.*, 2008, **20**, 691-695.
- G. Tourillon and F. Garnier, *J. Electrochem. Soc.*, 1983, **130**, 2042-2044.
- J. Roncali, *Chem. Rev.*, 1992, **92**, 711-738.
- M. Kobayashi, J. Chen, T.-C. Chung, F. Moraes, A. J. Heeger and F. Wudl, *Synth. Met.* 1984, **9**, 77-86.
- T.-C. Chung, J. H. Kaufman, A. J. Heeger and F. Wudl, *Phys. Rev. B*, 1984, **30**, 702-710.
- A. O. Patil, A. J. Heeger and F. Wudl, *Chem. Rev.*, 1988, **29**, 183-200.
- K. K. Kanazawa, A. F. Diaz, W. D. Gill, P. M. Grant and G. B. Street, *Synth. Met.*, 1980, **1**, 329-336.
- G. B. Street, T. C. Clarke, M. Krounbi, K. Kanazawa, V. Lee, P. Pfluger, J. C. Scott and G. Weiser, *Mol. Cryst. Liq. Cryst.*, 1982, **83**, 253-264.
- V. D. Mihailtchi, L. J. A. Koster, P. W. M. Blom, C. Melzer, B. de Boer, J. K. J. van Duren and R. A. J. Janssen, *Adv. Funct. Mater.*, 2005, **15**, 795-801.
- A. J. Berresheim, M. Müller and K. Müllen, *Chem. Rev.*, 1999, **99**, 1747-1785.
- I. F. Perepichka and D. F. Perepichka, Handbook of Thiophene-Based Materials, Wiley-VCH Press, Chichester, U.K., 2009.
- J. K. Politis, J. C. Nemes and M. David Curtis, *J. Am. Chem. Soc.*, 2001, **123**, 2537-2547.
- G. Distefano, D. Jones, M. Guerra, L. Favaretto, A. Modelli and G. Mengoli, *J. Phys. Chem.*, 1991, **95**, 9746-9753.
- K. Takimiya, Y. Kunugi, Y. Konda, N. Niihara and T. Otsubo, *J. Am. Chem. Soc.*, 2004, **126**, 5084-5085.
- G. R. Hutchison, M. A. Ratner and T. J. Marks, *J. Am. Chem. Soc.*, 2005, **127**, 16866-16881.
- T. L. Gilchrist, Heterocyclic Chemistry, Pitman Publishing, Ltd., London, 1985.

- 28 F. Bernardi, A. Bottoni and A. Venturini, *J. Mol. Struct. THEOCHEM*, 1988, **163**, 173-189.
- 29 M. K. Cyrański, T. M. Krygowski, A. R. Katritzky and P. v. R. Schleyer, *J. Org. Chem.*, 2002, **67**, 1333-1338.
- 30 A. Stanger, *J. Org. Chem.*, 2006, **71**, 883-893.
- 31 O. Gidron, A. Dadvand, E. Wei-Hsin Sun, I. Chung, L. J. W. Shimon, M. Bendikov and D. F. Perepichka, *J. Mater. Chem. C*, 2013, **1**, 4358-4367.
- 32 P. Sonar, S. P. Singh, E. L. Williams, Y. N. Li, M. S. Soh and A. Dodabalapur, *J. Mater. Chem.*, 2012, **22**, 4425-4435.
- 33 A. Gandini, *Macromolecules*, 2008, **41**, 9491-9504.
- 34 J. Binder and R. T. Raines, *J. Am. Chem. Soc.*, 2009, **131**, 1979-1985.
- 35 O. Gidron, A. Dadvand, Y. Sheynin, M. Bendikov and D. F. Perepichka, *Chem. Commun.*, 2011, **47**, 1976-1978.
- 36 M. J. Robb, S. Y. Ku, F. G. Brunetti and C. J. Hawker, *J. Polym. Sci. Part A: Polym. Chem.*, 2013, **51**, 1263-1271.
- 37 G. Tourillon and F. Garnier, *J. Electroanal. Chem.*, 1982, **135**, 173-178.
- 38 G. Zotti, G. Schiavon, N. Comisso, A. Berlin and G. Pagani, *Synth. Met.*, 1990, **36**, 337-351.
- 39 S. Glenis, M. Benz, E. LeGoff, J. L. Schindler, C. R. Kannewurf and M. G. Kanatzidis, *J. Am. Chem. Soc.*, 1993, **115**, 12519-12525.
- 40 X. B. Wan, F. Yan, S. Jin, X. R. Liu and G. Xue, *Chem. Mater.*, 1999, **11**, 2400-2407.
- 41 B. Nessakh, Z. Kotkowska-Machnik and F. Tedjar, *J. Electroanal. Chem.*, 1990, **296**, 263-268.
- 42 T. Ohsawa, K. Kaneto and K. Yoshino, *Jpn. J. Appl. Phys.*, 1984, **23**, L663.
- 43 F. Tediari, *Eur. Polym. J.*, 1985, **21**, 317-319.
- 44 R. Z. Li, X. J. Lv, D. Shi, D. F. Zhou, Y. M. Cheng, G. L. Zhang and P. Wang, *J. Phys. Chem. C*, 2009, **113**, 7469-7479.
- 45 J. T. Lin, P. C. Chen, Y. S. Yen, Y. C. Hsu, H. H. Chou and M. C. P. Yeh, *Org. Lett.*, 2009, **11**, 97-100.
- 46 B. Walker, A. B. Tomayo, X. D. Dang, P. Zalar, J. H. Seo, A. Garcia, M. Tantiwiwat and T. Q. Nguyen, *Adv. Funct. Mater.*, 2009, **19**, 3063-3069.
- 47 U. H. F. Bunz, *Angew. Chem., Int. Ed.*, 2010, **49**, 5037-5040.
- 48 Z. F. Chen, C. S. Wannere, C. Corminboeuf, R. Puchta and P. V. Schleyer, *Chem. Rev.*, 2005, **105**, 3842-3888.
- 49 O. Gidron, Y. Diskin-Posner and M. Bendikov, *J. Am. Chem. Soc.*, 2010, **132**, 2148-2150.
- 50 O. Gidron, N. Varsano, L.J.W. Shimon, G. Leituss and M. Bendikov, *Chem. Commun.*, 2013, **49**, 6256-6258.
- 51 E. Altunok, S. Friedle and S.W. Thomas, *Macromolecules*, 2013, **46**, 756-762.
- 52 J. Roncali and F. Garnier, *Synth. Met.*, 1986, **15**, 323-331.
- 53 G. E. Gunbas and A. Durmus, L. Toppare, *Adv. Mater.*, 2008, **20**, 691-695.
- 54 J. P. Parrish, V. L. Flanders, R. J. Floyd and K. W. Jung, *Tetrahedron Lett.*, 2001, **42**, 7729-7731.
- 55 R. C. Larock and J. C. Bernhardt, *J. Org. Chem.*, 1977, **42**, 1680-1684.
- 56 C. Zimmermann, M. Mohr, H. Zipse, R. Eichberger and W. Schnabel, *J. Photochem. Photobiol. A: Chem.*, 1999, **125**, 47-56.
- 57 C. L. Gaupp, D. M. Welsh, R. D. Rauh and J. R. Reynolds, *Chem. Mater.*, 2002, **14**, 3964-3970.
- 58 R.G. Parr and W. Yang, *Density Functional Theory of Atoms and Molecules*, Oxford University Press, New York, 1989.
- 59 G.A. Petersson and M.A. Al-Laham, *J. Chem. Phys* 1991, **94**, 6081-6090.
- 60 A.D. Becke, *Phys. Rev. A*, 1988, **38**, 3098-3100.
- 61 A.D. Becke, *J. Chem. Phys.*, 1993, **98**, 1372-1377.
- 62 A.D. Becke, *J. Chem. Phys.*, 1993, **98**, 5648-5652.
- 63 G.-G. Wu, H.O. Marcy, D.C. DeGroot, J.L. Schindler, C.R. Kannewurf, W.-Y. Leung, M. Benz, E. LeGoff and M.G. Kanatzidis, *Synth. Met.*, 1991, **41-43**, 797-803.
- 64 W.-Y. Leung and E. LeGoff, *Synth. Commun.*, 1989, **19**, 787-792.
- 65 J.G. Ji and X.Y. Lu, *J. Chem. Soc., Chem. Commun.*, 1993, 764-765.
- 66 J.W. McFarland, B.M. Howe, J.D. Lehmkuhler and D.C. Myers, *J. Heterocyclic. Chem.*, 1995, **32**, 1747-1750.
- 67 J.M. Kauffman and G. Moyna, *J. Heterocyclic. Chem.*, 2002, **39**, 981-988.
- 68 G. W. Lu and G. Q. Shi, *J. Electroanal. Chem.*, 2006, **586**, 154-160.
- 69 M. Zhou and J. Heinze, *Electrochim. Acta.*, 1999, **44**, 1733-1748.
- 70 I. Carrillo, E. Sánchez de la Blanca, M. J. González-Tejera and I. Hernández-Fuentes, *Chem. Phys. Lett.*, 1994, **229**, 633-637.
- 71 E. Sánchez de la Blanca, I. Carrillo, M. J. González-Tejera and I. Hernández-Fuentes, *J. Polym. Sci. Part A*, 2000, **38**, 291-298.
- 72 S. Sharma and M. Bendikov, *Chem. Eur. J.*, 2013, **19**, 13127-13139.
- 73 M. J. Gonzalez-Tejera, I. Carrillo and I. Hernandez-Fuentes, *Synth. Met.*, 1995, **73**, 135-140.
- 74 M. J. Gonzalez-Tejera, I. Carrillo and I. Hernandez-Fuentes, *Synth. Met.*, 1998, **92**, 187-195.
- 75 J. Roncali and F. Garnier, *Synth. Met.*, 1986, **15**, 323-331.
- 76 C. L. Gaupp, D. M. Welsh, R. D. Rauh and J. R. Reynolds, *Chem. Mater.*, 2002, **14**, 3964-3970.
- 77 G. Inzelt, M. Pineri, J. W. Schultze, M. A. Vorotyntsev, *Electrochim. Acta.*, 2000, **45**, 2403-2421.
- 78 D. Li, Y. P. Wen, J. K. Xu, H. H. He and M. Liu, *Chinese J. Polym. Sci.*, 2012, **30**, 705-718.
- 79 H.J. Nie, X.L. Chen, C.J. Yao, Y.W. Zhong, G.R. Hutchison and J. Yao, *Chem. Eur. J.*, 2012, **18**, 14497-14509.
- 80 B.Y. Lu, Y.Z. Li and J.K. Xu, *J. Electroanal. Chem.*, 2010, **643**, 67-76.
- 81 R. S. Becker, J. Seixas de Melo, A. L. Macüanita and F. Elisei, *J. Phys. Chem.*, 1996, **100**, 18683-18695.
- 82 J. K. Xu, H. T. Liu, S. Z. Pu, F. Y. Li and M. B. Luo, *Macromolecules*, 2006, **39**, 5611-5616.
- 83 M. L. Ma, H. T. Liu, J. K. Xu, Y. Z. Li and Y. Q. Wan, *J. Phys. Chem. C*, 2007, **111**, 6889-6896.
- 84 J. K. Xu, Y. J. Zhang, J. Hou, Z. H. Wei, S. Z. Pu, J. Q. Zhao and Y. K. Du, *Eur. Polym. J.*, 2006, **42**, 1154-1163.
- 85 F. Yukio, *J. Phys. Chem.*, 1996, **100**, 15644-15653.
- 86 S. Tirkés and A. M. Ónal, *J. Appl. Polym. Sci.*, 2007, **103**, 871-876.
- 87 S. Hotta, T. Hosaka and W. Shimotsuma, *J. Chem. Phys.*, 1984, **80**, 954-956.
- 88 R. McConnell, W. Godwin, B. Phillips, *J. Ark. Acad. Sci.*, 1997, **51**, 205-207.
- 89 S. Hotta, W. Shimotsuma and M. Taketani, *Synth. Met.*, 1984, **10**, 85-94.
- 90 S. Hotta, T. Hosaka, M. Soga and W. Shimotsuma, *Synth. Met.*, 1984, **10**, 95-99.
- 91 B. Y. Lu, J. Yan, J. K. Xu, S. Y. Zhou and X. J. Hu, *Macromolecules*, 2010, **43**, 4599-4608.
- 92 M.J. Gonzalez-Tejera, E. Sánchez de la Blanca and I. Carrillo, *Synth. Met.*, 2008, **158**, 165-189.
- 93 Y. C. Kung and S. H. Hsiao, *J. Mater. Chem.*, 2010, **20**, 5481-5492.
- 94 B.L. Funt and S.V. Lowen, *Synth. Met.*, 1985, **11**, 129-137.
- 95 O. Inganäs and B. Liedberg, *Synth. Met.*, 1985, **11**, 239-249.
- 96 G. Distefano, D. Jones, M. Guerra, L. Favaretto, A. Modelli and G. Mengoli, *J. Phys. Chem.*, 1991, **95**, 9746-9753.
- 97 T. A. Skotheim, R. L. Elsenbaumer and J. R. Reynolds, *Handbook of Conducting Polymers*, Marcel Dekker, Inc., New York, 1998.
- 98 K. Yoshino, Y. Kohno, T. Shirishi, K. Yoshino, Y. Kohno, T. Shirishi, K. Inoue and K. Tsukagoshi, *Synth. Met.*, 1985, **10**, 319-326.
- 99 G. Zotti, S. Martina, G. Wegner and A-D. Schliiter, *Adv. Mater.*, 1992, **4**, 798-801.
- 100 U. Salzner, J. B. Lagowski, P. G. Pickup and R. A. Poirier, *Synth. Met.*, 1998, **96**, 177-189.
- 101 P. M. Beaujuge and J. R. Reynolds, *Chem. Rev.*, 2010, **110**, 268-320.
- 102 J. Kim, J. You and E. Kim, *Macromolecules*, 2010, **43**, 2322-2327.
- 103 J. K. Politis, J. C. Nemes and M. D. Curtis, *J. Am. Chem. Soc.*, 2001, **123**, 2537-2547.
- 104 M. J. Gonzalez-Tejera, I. Carrillo and I. Hernandez-Fuentes, *Synth. Met.*, 1995, **73**, 135-140.
- 105 M. J. Gonzalez-Tejera and I. Carrillo, I. Hernandez-Fuentes, *Synth. Met.*, 1998, **92**, 187-195.